Article

SOURCE DATA | TRANSPARENT PROCESS | OPEN ACCESS

EMBO reports

Hepsin regulates TGFβ signaling via fibronectin proteolysis

Denis Belitškin[1], Shishir M Pant[1], Pauliina Munne[1], Ilida Suleymanova[1], Kati Belitškina[2], Hanna-Ala Hongisto[1], Johanna Englund[1], Tiina Raatikainen[1], Olga Klezovitch[3], Valeri Vasioukhin[3], Shuo Li[4], Qingyu Wu[4], Outi Monni[5], Satu Kuure[6], Pirjo Laakkonen[7], Jeroen Pouwels[1], Topi A Tervonen[1,†] & Juha Klefström[1,8,*,†]

Abstract

Transforming growth factor-beta (TGFβ) is a multifunctional cytokine with a well-established role in mammary gland development and both oncogenic and tumor-suppressive functions. The extracellular matrix (ECM) indirectly regulates TGFβ activity by acting as a storage compartment of latent-TGFβ, but how TGFβ is released from the ECM via proteolytic mechanisms remains largely unknown. In this study, we demonstrate that hepsin, a type II transmembrane protease overexpressed in 70% of breast tumors, promotes canonical TGFβ signaling through the release of latent-TGFβ from the ECM storage compartment. Mammary glands in hepsin CRISPR knockout mice showed reduced TGFβ signaling and increased epithelial branching, accompanied by increased levels of fibronectin and latent-TGFβ1, while overexpression of hepsin in mammary tumors increased TGFβ signaling. Cell-free and cell-based experiments showed that hepsin is capable of direct proteolytic cleavage of fibronectin but not latent-TGFβ and, importantly, that the ability of hepsin to activate TGFβ signaling is dependent on fibronectin. Altogether, this study demonstrates a role for hepsin as a regulator of the TGFβ pathway in the mammary gland via a novel mechanism involving proteolytic downmodulation of fibronectin.

Keywords breast cancer; fibronectin; hepsin; TGFβ; tumor microenvironment
Subject Categories Cancer; Cell Adhesion, Polarity & Cytoskeleton
DOI 10.15252/embr.202152532 | Received 27 January 2021 | Revised 4 August 2021 | Accepted 10 August 2021 | Published online 13 September 2021
EMBO Reports (2021) 22: e52532

Introduction

The human genome encodes 566 proteases, and of these, 273 have been found in extracellular compartments or the lumen of secretory compartments, 277 in intracellular compartments, and a small fraction at the plasma membrane (Overall & Blobel, 2007). Extracellular proteolysis plays a key role in regulating the physical properties of the extracellular matrix (ECM) through turnover, which, for example, affects branching morphogenesis in the mammary gland (Wiseman *et al*, 2003; Green & Lund, 2005; Lu *et al*, 2011). Another critical role of extracellular proteolysis lies in the processing of growth factor pro-forms (e.g., pro-HGF; Herter *et al*, 2005, pro-MSP Ganesan *et al*, 2011, and EGF Higashiyama *et al*, 2011). Therefore, extracellular proteolysis orchestrates the interaction between ECM remodeling and growth factor signaling during development and tissue regeneration (Mohammed & Khokha, 2005; Fukushima *et al*, 2018). Most studies on proteolytic regulation of the ECM have focused on the diverse class of matrix metalloproteinases (MMPs) (Chang & Werb, 2001). Interestingly, in addition to MMPs, serine proteases have been demonstrated to be involved in pericellular proteolysis of ECM components and plasma membrane proteins, allowing localized ECM remodeling and receptor signaling regulation (Del Rosso *et al*, 2002).

Hepsin is a protease belonging to the type II transmembrane serine protease (TTSP) family, a special group of membrane-anchored proteases whose enzymatic activity is confined to the pericellular space (Hooper *et al*, 2001), making TTSPs accessible for function-blocking antibodies and small molecule inhibitors (Antalis *et al*, 2010). Hepsin knockout mice display defects in inner ear development and have altered kidney function (Guipponi *et al*, 2007; Olinger *et al*, 2019). A recent study reported reduced liver size and browning of fat tissue in hepsin knockout mice, leading to a

1 Research Programs Unit/Translational Cancer Medicine Research Program and Medicum, Faculty of Medicine, Biomedicum Helsinki, University of Helsinki, Helsinki, Finland
2 Pathology Department, North Estonia Medical Centre, Tallinn, Estonia
3 Division of Human Biology, Fred Hutchinson Cancer Research Center, Seattle, WA, USA
4 Department of Cardiovascular and Metabolic Sciences, Lerner Research Institute, Cleveland Clinic, Cleveland, OH, USA
5 Research Programs Unit/Applied Tumor Genomics Research Program, Faculty of Medicine, Biomedicum Helsinki, University of Helsinki, Helsinki, Finland
6 GM-Unit, Laboratory Animal Centre, Helsinki Institute of Life Science (HiLIFE), University of Helsinki, Helsinki, Finland
7 Laboratory Animal Center, Helsinki Institute of Life Science (HiLIFE), University of Helsinki, Helsinki, Finland
8 Finnish Cancer Institute & FICAN South, Helsinki University Hospital (HUS), Helsinki, Finland
*Corresponding author. Tel.: +358294125493; E-mail: juha.klefstrom@helsinki.fi
†These authors contributed equally to this work as senior authors

reduction of body fat in mice on a high-fat diet (Li *et al*, 2020). Apart from a role for hepsin-mediated cleavage of pro-HGF in the liver (Hsu *et al*, 2012) and laminin-332 during invasion (Klezovitch *et al*, 2004; Tripathi *et al*, 2008; Pant *et al*, 2018a), the molecular mechanisms underlying other physiological functions of hepsin remain poorly defined.

Hepsin is one of the most frequently overexpressed proteins in prostate cancer (Dhanasekaran *et al*, 2001; Luo *et al*, 2001; Magee *et al*, 2001; Stamey *et al*, 2001; Welsh *et al*, 2001; Ernst *et al*, 2002; Chen *et al*, 2003; Stephan *et al*, 2004). Hepsin is also very frequently overexpressed in breast cancer, in up to 70% of breast tumors (Tervonen *et al*, 2016). Hepsin overexpression is suggested to promote cancer progression and metastasis (Tanimoto *et al*, 1997; Klezovitch *et al*, 2004; Tervonen *et al*, 2016), and several hepsin-regulated oncogenic pathways have been described. For example, overactive hepsin damages epithelial integrity and promotes degradation of the basement membrane (Klezovitch *et al*, 2004; Tripathi *et al*, 2008; Partanen *et al*, 2012; Tervonen *et al*, 2016), and hepsin directly cleaves oncogenic growth factors pro-HGF and pro-MSP (Herter *et al*, 2005; Ganesan *et al*, 2011). However, given that most proteases have a broad substrate range, additional signaling pathways downstream of hepsin probably exist that contribute to its oncogenic properties.

Here, we demonstrate that hepsin controls TGFβ signaling via proteolytic regulation of fibronectin. The findings are corroborated *in vivo* by using a new hepsin CRISPR knockout mouse model, alongside an established model of hepsin overexpression in breast cancer.

Results

CRISPR/Cas9-generated Hpn knockout mice manifest diminished liver size and partial loss of hearing

We generated hepsin knockout mice with CRISPR/Cas9-mediated gene editing using a guide RNA targeting exon 4 of the *Hpn* gene. Genetic analysis revealed a 50 bp frameshift deletion in the coding region of the *Hpn* gene (Fig 1A), which resulted in the loss of the hepsin protein in mice homozygous for the frameshift allele (Figs 1A and EV1A). *Hpn* knockout mice did not display any obvious histopathological changes, gross morphological, or tissue architecture deviations, nor did they show any differences in external appearance, lean mass, free fluid, or body fat (Fig EV1B–D). Consistent with *Hpn* knockout mice created via traditional homologous recombination methods (Wu *et al*, 1998; Li *et al*, 2020), our CRISPR hepsin knockout ($Hpn^{-/-}$) mice displayed diminished liver size and reduced hearing (Figs 1B and C, and EV1E).

$Hpn^{-/-}$ mice are deficient in TGFβ signaling in the mammary gland and show increased ductal branching

Hepsin is expressed in human and mouse epithelial tissues, where it typically localizes to desmosomal and hemidesmosomal junctions (Miao *et al*, 2008). Moreover, in the mammary gland, oncogenic deregulation of hepsin has been coupled to loss of epithelial integrity (Partanen *et al*, 2012; Tervonen *et al*, 2016). These findings prompted us to examine whether the loss of hepsin might affect signaling pathways relevant to cohesiveness or morphogenesis of the mammary epithelial tissue. Whole mammary glands were isolated from wild-type and $Hpn^{-/-}$ mice and analyzed in parallel by RNAseq and Reverse Phase Protein Array (RPPA). The RPPA analysis revealed *Hpn* knockout-specific changes in the levels of 12 proteins, including osteopontin, periostin, and endostatin (Fig EV2A and B). RNAseq analysis demonstrated that while the expression levels of mRNAs encoding 2 of these proteins were also altered, expression changes in other 10 proteins were not accompanied by corresponding changes in mRNA expression, suggesting that hepsin regulates proteomes via both transcription-associated and post-translational/proteolytic mechanisms (Fig EV2A–D).

Gene Set Enrichment Analysis (GSEA) was performed on the RNAseq data. Functional clustering of gene signatures affected by the absence of hepsin suggests the downregulation of TGFβ1 signaling in $Hpn^{-/-}$ mammary glands (Fig 1D and E, Table EV1). TGFβ signaling regulation occurs via two discrete activation steps: the processing of latent-TGFβ in the extracellular compartment and TGFβ receptor-induced activation of downstream signaling, which includes phosphorylation of receptor-associated Smads (R-Smads), such as Smad2 and Smad3 (Derynck & Budi, 2019). To confirm the downmodulation of TGFβ signaling in $Hpn^{-/-}$ mice, we determined

Figure 1. The knockout of hepsin with CRISPR/Cas9 inhibits TGFβ signaling in the mouse mammary gland.

A Hepsin knockout mice harbor a 50 bp frameshift deletion in the 4th exon of the *Hpn* gene (TM = transmembrane domain, SRCR = scavenger receptor cysteine-rich domain, SPD = serine protease domain; red bar indicates gRNA-binding site). Immunoblot from whole mammary lysates against hepsin protein ($Hpn^{+/+}$ = Wt, $Hpn^{+/-}$ = heterozygous deletion, $Hpn^{-/-}$ = homozygous deletion) (representative of 3 mice per group).

B Weight of indicated organs isolated from Wt ($N = 3$) and $Hpn^{-/-}$ ($N = 4$) mice.

C Acoustic startle reflex test to compare hearing ability between Wt ($N = 7$) and $Hpn^{-/-}$ ($N = 4$) mice.

D Cytoscape enrichment map of pathways affected in $Hpn^{-/-}$ whole mammary glands compared with Wt controls ($N = 3$ per group). Node size correlates with the number of genes in the signature; node color correlates with either gene set enrichment (red) or reduction (blue) in $Hpn^{-/-}$ mammary glands. A full list of gene signatures affected in $Hpn^{-/-}$ mammary glands is shown in Table EV1.

E Gene Set Enrichment Analysis (GSEA) graphs showing enrichment of indicated TGFβ1 signaling gene sets in $Hpn^{-/-}$ mammary glands compared with Wt mammary glands (FDRp—*P*-value; FWERq—false discovery rate; NES—normalized enrichment score).

F Immunoblot analysis of phospho-Smad2/3 (TGFβ pathway signaling marker) and total Smad2/3 in lysates from indicated tissues isolated from Wt, $Hpn^{+/-}$, and $Hpn^{-/-}$ mice. GAPDH was used as the loading control. The histogram depicts quantification of pSmad2/3 compared to Wt, normalized to total Smad2/3.

G Representative Carmine alum stained mammary gland whole mounts from Wt and $Hpn^{-/-}$ mice. The histogram depicts quantification of duct length normalized to duct length in Wt mammary glands. The scale bar represents 1 mm. Data in (B, C, F, G) are represented as mean ± SD, and Student's *t*-test was used for statistical analyses.

Source data are available online for this figure.

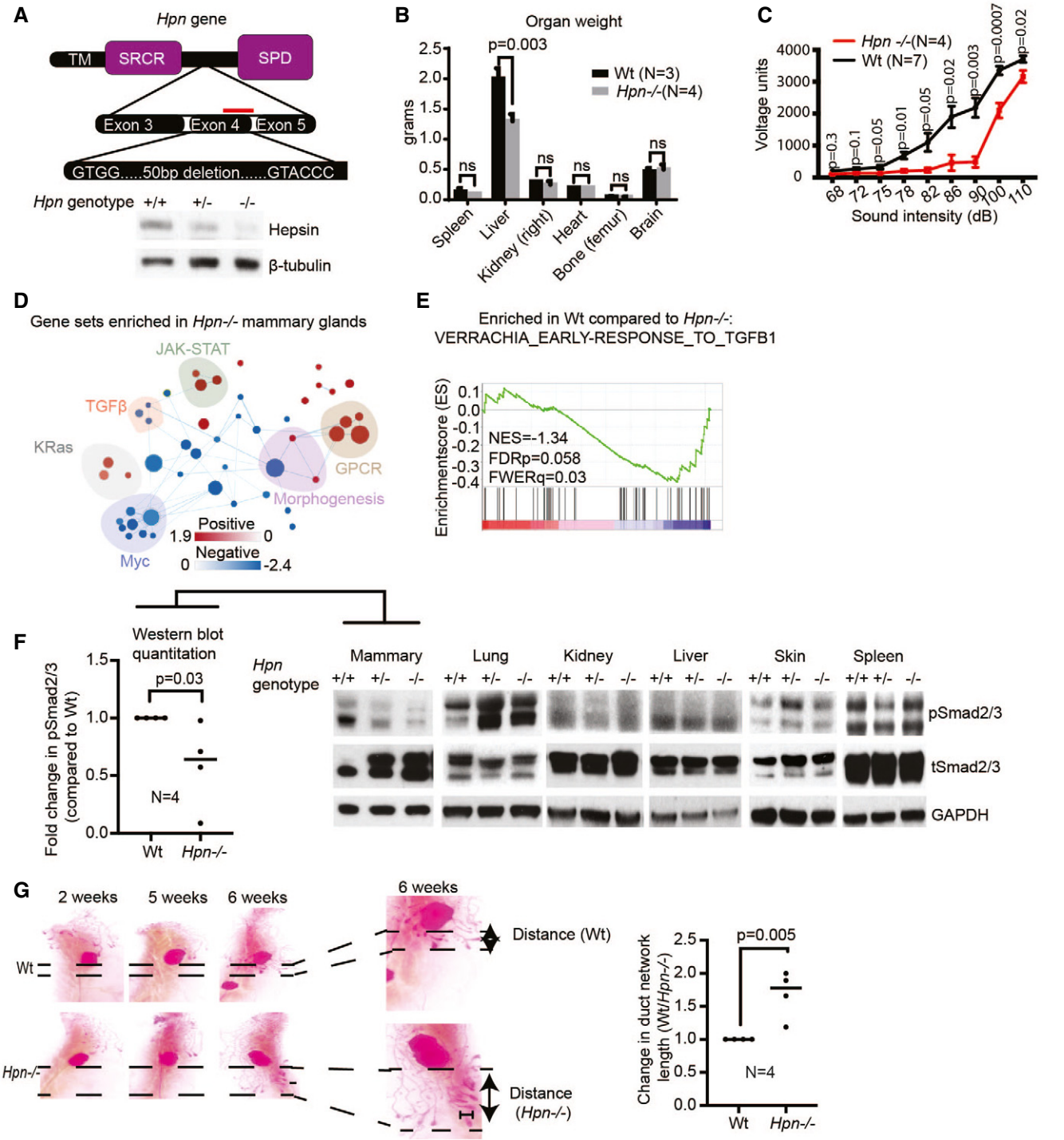

Figure 1.

the levels of phospho-Smad2/3 in tissue extracts from mammary, lung, kidney, liver, skin, and spleen. The level of phosphorylated Smad2/3 was significantly decreased in $Hpn^{-/-}$ mammary tissue (Fig 1F), indicating deficient canonical TGFβ signaling in the mammary gland upon loss of hepsin. Reduced phosphorylated Smad2/3 levels were not observed in the other tissues examined (Fig 1F), suggesting that this phenomenon is specific to the mammary gland.

TGFβ is a well-established suppressor of mammary duct branching and proliferation (Ewan *et al*, 2002; Ingman & Robertson, 2008; Moses & Barcellos-Hoff, 2011). Analysis of mammary gland whole mounts from 6-week-old wild-type and $Hpn^{-/-}$ littermates showed

that loss of hepsin increased duct branching into the fat pad (Fig 1G). This phenotype resembles the one observed in TGFβ1$^{+/-}$ mice (Ewan *et al*, 2002; Ingman & Robertson, 2008), thus showing that loss of hepsin affects mammary morphogenesis in a manner consistent with reduced TGFβ signaling.

Hepsin overexpression activates TGFβ signaling in a Wap-Myc model of breast cancer

The TGFβ pathway is commonly dysregulated in human cancer but its impact on tumorigenesis is highly contextual—while TGFβ has tumor-suppressive effects, it also exerts pro-tumorigenic effects by modulating processes such as cell invasion, production of ECM, and inflammatory immune responses (Yeung *et al*, 2013; Bellomo *et al*, 2016; Mariathasan *et al*, 2018; Tauriello *et al*, 2018). To test whether ectopic overexpression of hepsin induces TGFβ signaling in the context of tumorigenesis, we made use of a previously published tumor syngraft model of Myc-driven breast cancer (Partanen *et al*, 2012; Utz *et al*, 2020). Wap-Myc mammary tumor cells, which express high Myc levels, were isolated from donor mice, transduced with the pIND21-HPN lentiviral construct that allows doxycycline (DOX)-induced hepsin overexpression (Tervonen *et al*, 2016), and subsequently transplanted into recipient mice (Fig 2A). Consistent with the notion that hepsin promotes TGFβ signaling, Western blot analysis revealed increased phospho-Smad2/3 and upregulation of the TGFβ signaling downstream target SNAIL in Wap-Myc tumors with DOX-induced hepsin overexpression compared with control (DOX$^-$) tumors (Fig 2B). RNAseq analysis of these tumors provided additional evidence for TGFβ pathway upregulation by hepsin as the most significantly upregulated gene signatures corresponded to the TGFβ signaling pathway (Figs 2C, D, and E, and EV3A and B). The largest cluster of gene signatures affected by hepsin overexpression, however, was related to the ECM and integrins (Fig 2C).

Hepsin regulates the extracellular activation of TGFβ signaling

Pro-TGFβ protein, which consists of both the mature TGFβ and latency-associated peptide (LAP), is released from cells in a latent form. This so-called TGFβ small latent complex (SLC) consists of the receptor-binding TGFβ growth factor dimer (12 kDa Western blot band under reducing conditions) and a dimer of the latency-associated peptide (LAP) (40 kDa Western blot band under reducing conditions) (Miyazono *et al*, 1988), where LAP inhibits the TGFβ growth factor dimer from binding and activating TGFβ receptors. The latent-TGFβ SLC is stored in the ECM through a covalent bond between LAP and latent-TGFβ-binding protein (LTBP), forming the large latent complex (LLC), which binds to fibronectin and fibrillins (Fig 3A) schematically depicts the TGFβ-LAP-LTBP complex). TGFβ can be released from LAP-LTBP, and thus from ECM storage, and activated by multiple types of stimuli, such as reactive oxygen species, proteases, or an acidic environment (Lyons *et al*, 1988, 1990; Sato & Rifkin, 1989; Yu & Stamenkovic, 2000; Jenkins, 2008; Sounni *et al*, 2010; Liu & Desai, 2015). Active TGFβ then mediates the tetramerization of type II TGFβ receptor (TGFβR2) and type I TGFβ receptor (TGFβR1), leading to phosphorylation of downstream receptor-associated R-Smads. Subsequently, phosphorylated R-Smads form oligomeric complexes with other Smads and translocate to the nucleus to regulate the transcription of target genes (Derynck & Budi, 2019).

Interestingly, further comparison of protein lysates from Wt and *Hpn*$^{-/-}$ mammary glands exposed markedly increased levels of LAP in *Hpn*$^{-/-}$ mammary glands, indicating accumulation of latent-TGFβ (Fig 3B). *Tgfb1* mRNA levels were not altered by the loss of hepsin (Fig EV3C), suggesting that these effects are due to post-transcriptional events. To find further evidence for accumulation of latent-TGFβ, we syngrafted Wt Wap-Myc tumor cells into the fat pads of either Wt or *Hpn*$^{-/-}$ syngeneic hosts (Fig 3C) and measured phospho-Smad2/3 levels in tumor lysates. In this experiment, we observed increased phospho-Smad2/3 levels in tumors grown in *Hpn*$^{-/-}$ mice (Fig 3D), consistent with a model where latent-TGFβ1 accumulates in ECM stores in mammary glands in the absence of hepsin and processed TGFβ1 is liberated by tumor cells, leading to activation of the TGFβ1 pathway. While these results leave room for several other interpretations, at this stage they prompted us to investigate two possible lines of inquiry: (i) Hepsin or one or more proteases regulated by hepsin could directly cleave LAP, which releases active TGFβ from SLC, or (ii) hepsin could be needed for the release of latent-TGFβ from ECM stores, after which hepsin-independent processes convert latent-TGFβ into its active form.

To address whether hepsin directly or indirectly contributes to proteolytic processing of latent-TGFβ1 LAP in cells, we performed several assays using the MCF10A-pIND20-HPN cell line (Tervonen *et al*, 2016). We established that DOX-induced ectopic hepsin expression enhances Smad2/3 phosphorylation in this cell line (Fig 3E), thus demonstrating its suitability to model hepsin-mediated regulation of TGFβ1 signaling. Importantly, hepsin-induced phosphorylation of Smad2/3 was rescued by the TGFβR1 inhibitor galunisertib, confirming that the hepsin-induced changes in pSmad2/3 levels were dependent on TGFβ receptor signaling (Fig 3E). First, we tested whether hepsin overexpression increases proteolytic processing of the inhibitory LAP peptide by incubating MCF10A-pIND20-HPN cells, with (DOX$^+$) and without (DOX$^-$) hepsin overexpression, with purified latent-TGFβ1 (LAP-TGFβ; SLC) for 24 h before harvesting conditioned medium and cell extracts for Western blotting (Fig 3F). No cleavage of the full-length LAP peptide was observed upon hepsin overexpression, indicating that hepsin does not affect proteolytic processing of the LAP peptide. Secondly, we examined whether adding exogenous latent-TGFβ1 further potentiates hepsin-induced PAI-1 induction in MCF10A-pIND20-HPN cells (Fig EV3D and E). While hepsin overexpression and treatment with exogenous latent-TGFβ each enhanced TGFβ receptor signaling (PAI-1 expression was used as a readout (Cichon *et al*, 2016)), the combination of hepsin overexpression and latent-TGFβ did not have an additive effect (Fig EV3D), further suggesting that hepsin does not stimulate extracellular cleavage of TGFβ1 LAP. Thirdly, using a TGFβ ELISA assay (Brown *et al*, 1990), we measured active and total TGFβ levels in conditioned medium from TGFβ1-overexpressing MCF10A-pIND20-HPN cells with (DOX$^+$) or without (DOX$^-$) hepsin overexpression (Fig 3G). While this TGFβ ELISA assay only detects active TGFβ1 (Brown *et al*, 1990), we utilized heat treatment of the conditioned medium to activate all TGFβ1 and thus to effectively measure total TGFβ1 levels. If hepsin would directly or indirectly promote cleavage of the LAP peptide, we expect hepsin overexpression to increase active TGFβ1 levels in

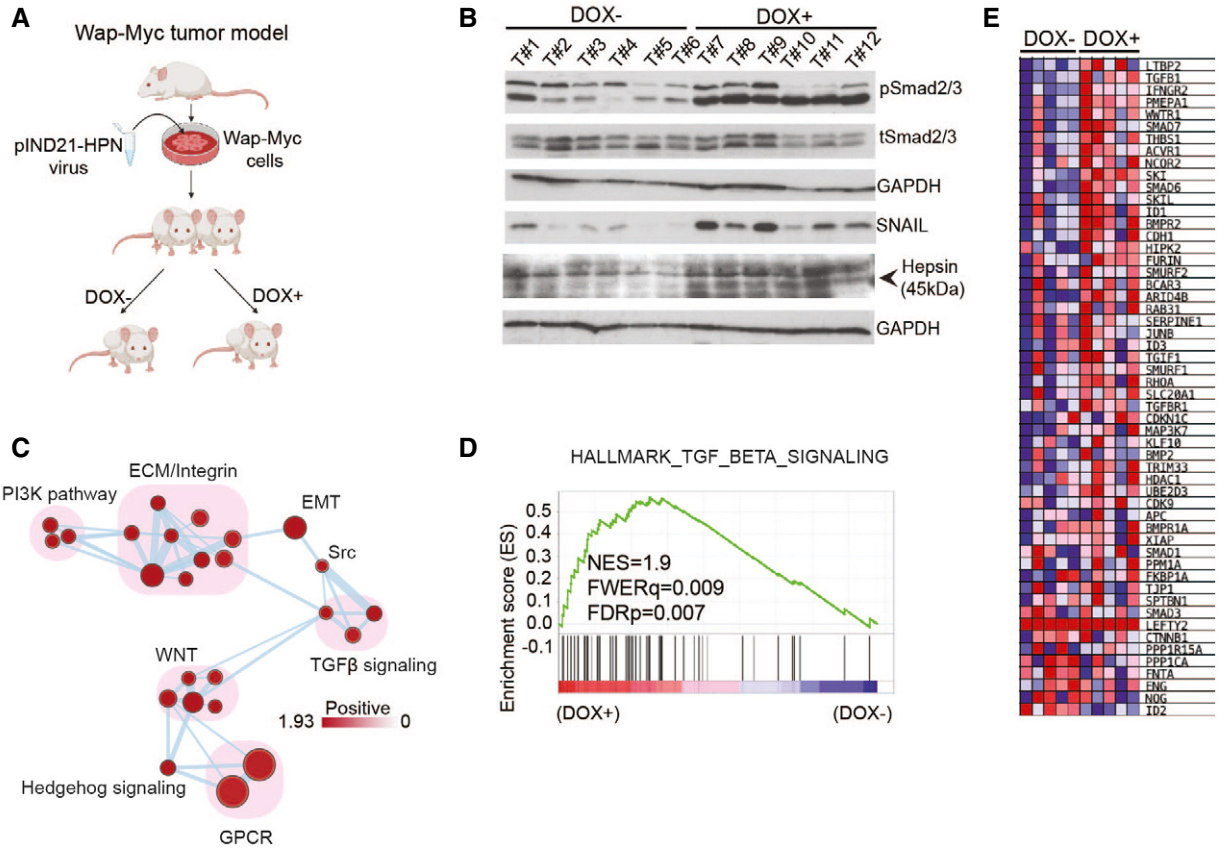

Figure 2. Overexpression of *Hpn* in Wap-Myc-driven mammary tumors induces TGFβ signaling.

A Schematic representation of the mouse experiment.

B Immunoblot analysis of Wap-Myc mammary tumor lysates for the indicated TGFβ signaling markers and hepsin (T# denotes individual tumors). GAPDH was used as the loading control. Lysates were derived from Wap-Myc mammary tumors from six mice with and six mice without DOX-induced hepsin overexpression (see (A)).

C Gene Set Enrichment Analysis (GSEA) enrichment map of pathways upregulated in hepsin overexpressing Wap-Myc tumors (DOX^+) compared with control tumors (DOX^-) ($N = 5$ tumors in each group). Node size correlates with the number of genes in the signature; node color red correlates with enrichment in hepsin overexpressing Wap-Myc tumors.

D GSEA graph comparing the expression of the HALLMARK_TGF_BETA_SIGNALING gene set in hepsin overexpressing (DOX^+) to control (DOX^-) Wap-Myc tumors ($N = 5$ tumors per group; FDRp—*P*-value; FWERq—false discovery rate; NES—normalized enrichment score).

E Heatmap showing changes in expression of all genes in the HALLMARK_TGF_BETA_SIGNALING gene set in hepsin overexpressing (DOX^+) compared with control (DOX^-) Wap-Myc tumors. Red color indicates upregulation, and blue color indicates the downregulation of the indicated genes.

the conditioned medium, i.e., released from the insoluble ECM. We did not observe such an increase in active TGFβ1 levels (Fig 3G; first 2 columns), however, providing additional evidence that hepsin does not affect cleavage of TGFβ1 LAP. We did, however, observe a modest but significant increase in total TGFβ (after heat activation of TGFβ) in the conditioned medium of hepsin overexpressing cells (Fig 3G; last 2 columns), which is consistent with the second hypothesis mentioned above, i.e., that hepsin could be needed for the release of latent-TGFβ from ECM stores. Lastly, we performed an *in vitro* protease assay, which showed that recombinant hepsin is unable to proteolytically process recombinant latent-TGF-β1 LAP (Fig 3H), suggesting that hepsin does not directly cleave LAP.

Together, the experiments in Figs 3B, E–H, and EV3D strongly suggest that hepsin causes accumulation of latent-TGFβ1 and promotes TGFβ signaling via mechanisms other than direct proteolytic cleavage of latent-TGFβ.

Hepsin downregulates the levels of ECM protein fibronectin

To identify hepsin-regulated ECM proteins, we examined both lysates and culture supernatants collected from MCF10A-pIND20-HPN cells with or without hepsin overexpression. The lysates and supernatants were separated on SDS–PAGE under reducing or non-reducing conditions followed by Coomassie staining, which revealed eight protein bands visibly affected by hepsin overexpression (Fig 4A). These proteins were analyzed by mass spectrometry, identifying fibronectin (FN1) as one of the proteins showing reduced expression in culture supernatant upon hepsin overexpression (Fig 4A). Hepsin-dependent downmodulation of fibronectin was of great interest, given the well-established role for fibronectin in the storage of TGFβ family growth factors, and thus in TGFβ signaling (Dallas *et al*, 2005; Robertson *et al*, 2015). Immunoblotting of the cell culture supernatant from the same cells showed accumulation

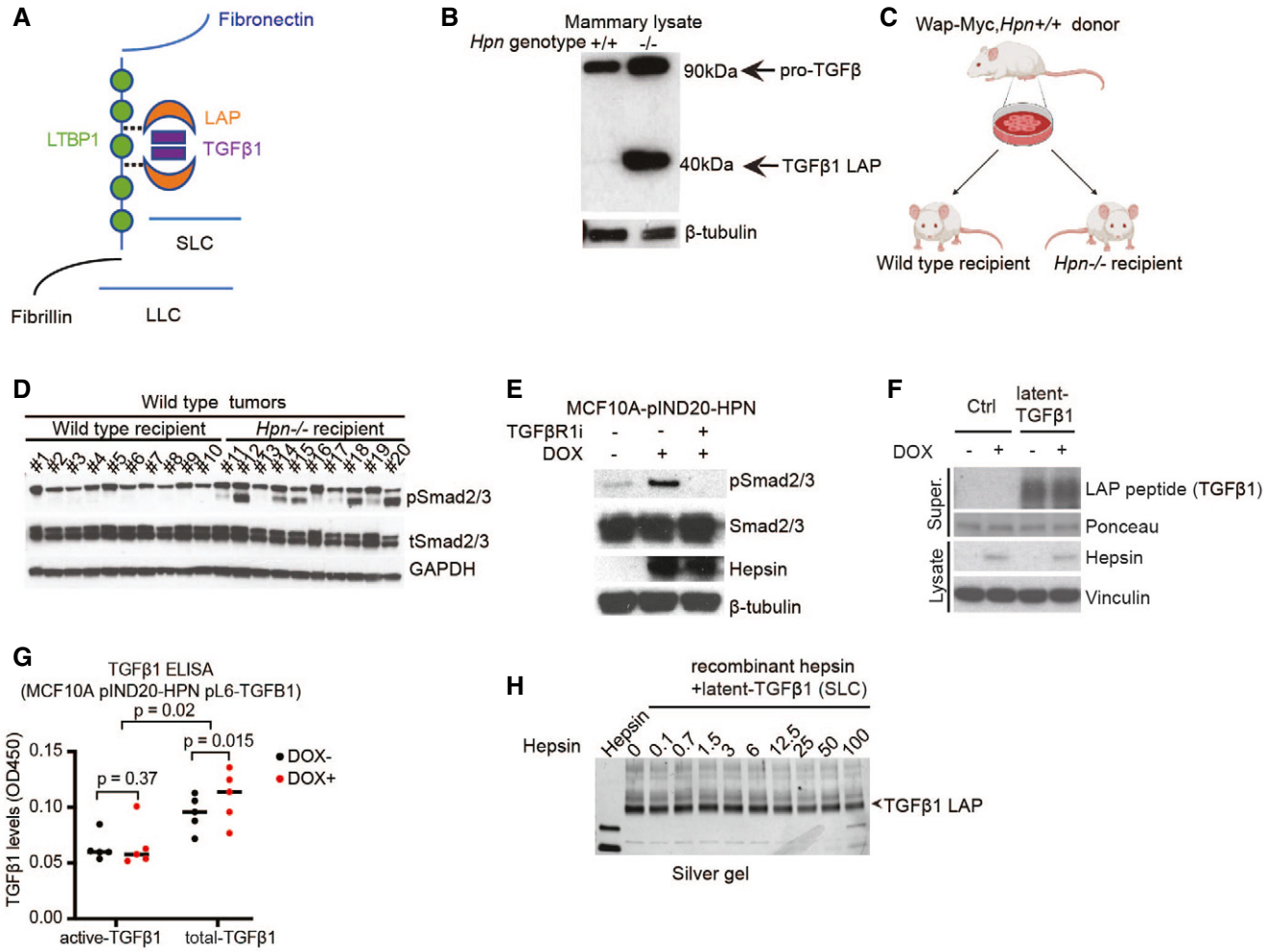

Figure 3. Hepsin is a regulator of TGFβ storage.

A Schematic illustration of proteins involved in TGFβ storage in the extracellular matrix. The small latent complex (SLC) is a non-covalently linked tetramer of 2 LAP (latency-associated peptide) (40 kDa) and 2 TGFβ1 (12 kDa). LTBP1 + SLC together form the large latent complex (LLC) through covalent bonds between LAP and LTBP1. LLC interacts with the ECM through non-covalent interactions of LTBP with fibrillins and fibronectin.

B Immunoblot analysis of LAP in mammary whole tissue lysates from Wt and $Hpn^{-/-}$ mouse. The 90 kDa band represents unprocessed pro-TGFβ, and the 40 kDa band corresponds to mature TGFβ LAP peptide.

C Schematic representation of the mouse experiment, showing orthotopic transplantation of Wt Wap-Myc tumor cells into syngeneic Wt and $Hpn^{-/-}$ recipients.

D Immunoblot analysis of phospho-Smad2/3, total Smad2/3, and GAPDH (loading control) expression in Wt tumors transplanted into either Wt or $Hpn^{-/-}$ recipients ($N = 10$ tumors each).

E Western blot analysis of phospho-Smad2/3, total Smad2/3, hepsin, and β-tubulin (loading control) in MCF10A-pIND20-HPN cells treated with 1 μg/ml doxycycline for 48 hours (DOX; overexpression of hepsin) and the TGFβR1 inhibitor galunisertib (TGFβR1i, 10 μM) as indicated.

F Immunoblot analysis of conditioned medium (LAP peptide) and cell extracts (hepsin and vinculin) from control (DOX) or hepsin overexpressing (DOX^+) MCF10A-pIND20-HPN supplemented with 100 ng/ml latent-TGFβ (small latent complex). Ponceau was used as a loading control for the cell culture medium.

G TGFβ ELISA assay to detect active and total TGFβ levels in conditioned medium from MCF10A-pIND20-HPN pL6-TGFβ1 cells with (DOX^+) or without (DOX^-) hepsin overexpressing. The TGFβ ELISA assay detects active TGFβ levels (first 2 columns), but heat treatment of the conditioned medium activates all TGFβ, thus effectively measuring total TGFβ (right two columns). Data are presented as scatter plot (mean denoted by the black line), and paired Student's *t*-test was used for statistical analyses.

H Silver-stained protein gel with samples from an *in vitro* protease activity assay with recombinant SLC and hepsin. SLC was incubated with increasing concentrations of recombinant hepsin (numbers indicate the concentration of hepsin in nM). Western blots in (B, E, F) are representative of at least three repeats.

of lower MW fibronectin fragments upon hepsin overexpression, which could indicate that reduced fibronectin levels in the cell extracts are due to fibronectin degradation (Fig 4B). Immunoblot for fibronectin in lysates of MCF10A-pIND20-HPN cells with or without hepsin overexpression confirmed the reduction in full-length fibronectin levels upon hepsin overexpression (Fig 4C).

To determine whether fibronectin could be a target for direct proteolytic processing by hepsin, we performed *in vitro* cleavage assays with purified proteins. This experiment showed that hepsin can cleave full-length fibronectin *in vitro* (Fig 4D, upper panel). Using different N-terminal and C-terminal fragments, we mapped the hepsin cleavage site to the N-terminal 70 kDa part of fibronectin

(Figs 4D, lower panel, and EV3F–J). While the *in vitro* cleavage assays exposed only one direct hepsin cleavage site in fibronectin, we note that hepsin overexpression induced a smear-like pattern of extracellular fibronectin cleavage products in MCF10A-pIND20-HPN cell culture supernatant (Fig 4B). Thus, it is likely that other proteases downstream of hepsin also contributed to hepsin-dependent fibronectin degradation.

Next, we investigated whether hepsin also downmodulates fibronectin *in vivo*. To that end, we analyzed a panel of tissue samples from our wild-type (Wt) and $Hpn^{-/-}$ mice. The results showed that $Hpn^{-/-}$ mammary glands, and also skin, expressed more fibronectin protein than mammary glands from Wt littermates (Fig 5A). Similar effects were not observed in other examined tissues (Fig 5A). Importantly, the increased fibronectin protein abundance in the $Hpn^{-/-}$ mammary glands was not accompanied by increased *Fn1* mRNA expression (Fig EV3K). An inverse correlation between fibronectin and hepsin was also observed in mammary glands from another hepsin knockout mouse strain (Wu *et al*, 1998) (Fig 5B) and in prostate tissue from mice genetically engineered to overexpress hepsin specifically in the prostate gland (Klezovitch *et al*, 2004) (Fig 5C). Together, our findings demonstrate that hepsin downregulates fibronectin protein levels in cultured cells and *in vivo*.

Hepsin regulates TGFβ1 signaling via fibronectin

If our hypothesis that hepsin activates TGFβ signaling through degradation of fibronectin is correct, downregulation of fibronectin should be sufficient to increase TGFβ signaling. We assessed this using four different experiments. We silenced fibronectin in MCF10A-pIND20-HPN cells and assessed TGFβ signaling using Western blot for pSmad2/3. Consistent with our hypothesis, downmodulation of fibronectin levels in these cells was sufficient to increase pSmad2/3 levels (Figs 6A and EV4A shows uncut immunoblot). In an MCF10A cell line overexpressing TGFβ-V5, silencing of fibronectin released the fully processed V5-tagged TGFβ (12 kDa) into the culture medium and also upregulated Smad2/3 phosphorylation (Figs 6B and EV4B shows uncut immunoblot). In addition, we performed a TGFβ1 reporter assay for which we created the MCF10A-pIND20-HPN pL6-TGFβ1 (SRE) TGFβ1 reporter cell line, harboring a construct with luciferase under the control of a Smad-response element (SRE). In line with our hypothesis that fibronectin modulates TGFβ signaling, silencing fibronectin, as well as induction of hepsin expression, in this cell line increased TGFβ1 reporter activity (Figs 6C and EV4D). Lastly, we verified that knockdown of fibronectin leads to TGFβ release into the culture supernatant using a breast cancer cell line (Hs578T) that expresses high levels of endogenous TGFβ (Figs 6D and EV4C). Together, these findings suggest that reducing fibronectin levels is sufficient to promote TGFβ release from the extracellular matrix and activate signaling, consistent with our hypothesis that hepsin promotes TGFβ signaling through fibronectin degradation.

If hepsin-dependent TGFβ pathway activation is due to fibronectin proteolysis, reduced fibronectin levels should dampen hepsin-induced TGFβ signaling activation. To investigate this, we examined the effect of fibronectin silencing on hepsin-dependent induction of pSmad2/3 in MCF10A-pIND20-HPN cells. We found that in the absence of fibronectin, hepsin shows reduced capacity to activate TGFβ signaling indicated by pSmad2/3 levels (Fig 6E). These results were confirmed using a TGFβ1 reporter assay with control or fibronectin silenced MCF10A-pIND20-HPN pL6-TGFβ1 (SRE) TGFβ1 reporter cells with (DOX^+) or without (DOX^-) hepsin overexpression (Fig 6F). Importantly, a TGFβ titration experiment with the MCF10A-pIND20-HPN pL6-TGFβ1 (SRE) TGFβ1 reporter cell line showed that incubation with low levels (0.01 ng/ml) of TGFβ1 increased SRE reporter activity by approximately 30% (Fig EV4E), similar to the increased SRE reporter activity induced by silencing FN1 (Fig 6C) or DOX-induced hepsin expression (Fig 6F). Similar to the experiments with silencing FN1 (Fig 6B) or DOX-induced hepsin expression (Fig 6E), this 0.01 ng/ml of TGFβ1 induced robust induction of pSMAD2/3 levels in this cell line (Fig EV4F), thus providing evidence that the changes in SRE reporter activity and pSMAD2/3 levels are in concordance.

Together, our results demonstrate that hepsin-mediated TGFβ signaling depends on fibronectin, consistent with a role for hepsin in fibronectin degradation and subsequent activation of latent-TGFβ (see a schematic model in Fig 6G).

Discussion

In this study, we identified the protease hepsin as a promoter of TGFβ signaling in the mammary gland and mammary tumors. We provide evidence that hepsin promotes TGFβ signaling through downregulation of fibronectin levels and subsequent release of latent-TGFβ from the ECM storage compartment.

The oncogenic role of hepsin overexpression has been well-established (Klezovitch *et al*, 2004; Tervonen *et al*, 2016), but the mechanisms through which hepsin promotes initiation and progression of tumors are still largely unclear. The especially frequent hepsin overexpression in breast cancer (up to 70% (Tervonen *et al*, 2016)) warrants further studies of the role of hepsin in mouse models of breast cancer. To facilitate such studies, we generated a new hepsin knockout mouse in the inbred FVB/N strain using CRISPR/Cas9 gene editing, since many common mouse models of breast cancer designed to study multistage carcinogenesis, such as MMTV-PyT (directs polyomavirus middle T antigen to mammary tissue), C3(1)-Tag (drives SV40 large T antigen to prostate and mammary tissue), and Wap-Myc (directs Myc to luminal mammary epithelial cells), have been generated in this strain. We anticipate that these $Hpn^{-/-}$ mice will facilitate future studies aimed to clarify the role of hepsin in multistage tumorigenesis through syngraft approaches, as presented here (Fig 3C).

The FVB/N $Hpn^{-/-}$ mice displayed hearing loss and reduced liver size, consistent with the phenotypes reported for earlier hepsin knockout mouse models (Guipponi *et al*, 2007; Li *et al*, 2020), demonstrating the validity of our knockout model. In addition to these phenotypes, we observed increased epithelial branching in $Hpn^{-/-}$ mammary glands. This novel mammary gland phenotype resembles the phenotype reported for $Tgf\beta^{+/-}$ females, which show a branching phenotype at the age of 6 weeks (Ewan *et al*, 2002; Ingman & Robertson, 2008). $Tgf\beta^{-/-}$ mice develop multiple severe phenotypes, such as neurodegeneration, developmental defects, and autoimmunity (Shull *et al*, 1992; Kulkarni *et al*, 1993; Dickson *et al*, 1995; Proetzel *et al*, 1995; Sanford *et al*, 1997; Brionne *et al*, 2003). The absence of these phenotypes in $Hpn^{-/-}$ knockout mice shows that hepsin is not required for overall TGFβ function *in vivo* but it is

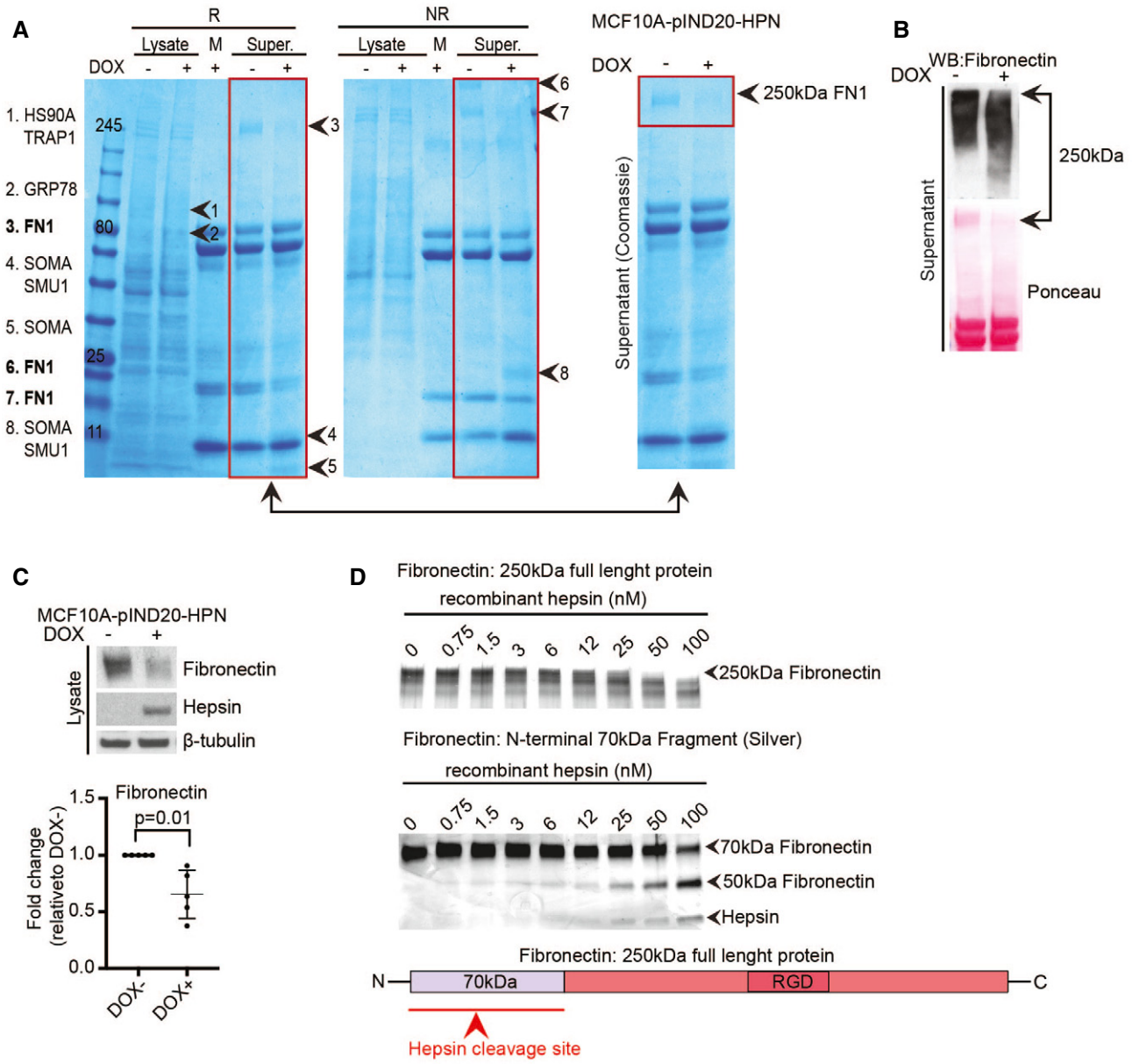

Figure 4. Hepsin promotes the proteolytic processing of fibronectin.

A Coomassie-stained protein gels with cell lysates and concentrated culture supernatants of MCF10A-pIND20-HPN cells, with (DOX^+) or without (DOX^-) hepsin overexpression. M indicates the media only control. R and NR above the gels indicate reducing and non-reducing conditions, respectively. Numbered arrowheads indicate areas of the gel that were analyzed by mass spectrometry; corresponding proteins differently expressed in hepsin overexpressing cells are listed on the left. The image with two lanes on the right is a copy of the indicated area with supernatant under reducing conditions, highlighting the part from which fibronectin was identified. Red boxes indicate the lanes that were analyzed by mass spectrometry.

B Immunoblot analyses of fibronectin expression in concentrated culture supernatant from MCF10A-pIND20-HPN cells with (DOX^+) or without (DOX^-) hepsin overexpression. Ponceau staining of the Western blot is shown as the loading control.

C Immunoblot analysis of fibronectin, hepsin, and β-tubulin (loading control) in cell lysates from MCF10A-pIND20-HPN cells with (DOX^+) or without (DOX^-) hepsin overexpression. The graph shows the quantification of fibronectin levels. Student's *t*-test was used for statistical analyses. Data are represented as mean ± SD.

D Silver-stained protein gel with samples from an *in vitro* protease activity assay with recombinant hepsin and either full length purified plasma fibronectin (upper panel) or the 70 kDa most N-terminal fragment of fibronectin (lower panel). Full-length fibronectin (1 μg) or the 70 kDa fibronectin fragment (1 μg) was incubated with increasing concentrations of recombinant hepsin. Arrowheads indicate full-length fibronectin, the 70 kDa fragment, the 50 kDa cleavage fragment generated by hepsin, and hepsin. The schematic figure shows the full-length fibronectin protein and the 70 KDa N-terminal fragment. The red arrow indicates the location of the putative hepsin cleavage site. RGD indicates the RGD-binding domain in fibronectin. Experiments in (B, C, D) are representative of at least three repeats.

Source data are available online for this figure.

plausible that hepsin is either a tissue-specific regulator of TGFβ function or that other proteases compensate the loss of hepsin outside the mammary gland. This selective role of hepsin in the regulation of extracellular TGFβ signaling opens up possibilities to modulate the TGFβ pathway in a mammary tissue-selective manner with the existing neutralizing antibodies or small molecule inhibitors of hepsin (Ganesan *et al*, 2012; Koschubs *et al*, 2012; Pant *et al*, 2018b; Damalanka *et al*, 2019).

TGFβ signaling is regulated by the ECM, in which three components are directly involved in the storage of latent-TGFβ: LTBPs, fibrillins, and fibronectin (ten Dijke & Arthur, 2007). Interestingly, some human conditions caused by dysregulation of TGFβ signaling are linked either to genetic alterations of TGFβ-binding fibrillins, or proteolytic alterations of LTBPs, indicating that release of the growth factor complex from the ECM may regulate pathway activation and provide a niche for a tissue-specific regulatory layer (Neptune *et al*, 2003; Ge & Greenspan, 2006; Quarto *et al*, 2012; Beaufort *et al*, 2014).

One important mechanism to activate latent-TGFβ is mediated by integrins (Robertson & Rifkin, 2016), which can bind LAP/LTBP and activate TGFβ by either pulling latent-TGFβ apart through mechanical forces generated by the actin cytoskeleton that are transmitted to the fibronectin-containing ECM by the integrins or presenting latent-TGFβ to metalloproteases for proteolytic cleavage (Fontana *et al*, 2005; Mamuya & Duncan, 2012). In addition to integrin-mediated TGFβ activation, various integrin-independent TGFβ activation pathways are known, for example, through reactive oxygen species, pH, and proteolytic cleavage (Robertson & Rifkin, 2016). Our data identify hepsin as a novel activator of TGFβ signaling that mediates the release of latent-TGFβ from the ECM (Fig 2A–G) through degradation of fibronectin (Fig 6A–F) and does not activate TGFβ signaling through direct or indirect cleavage of LAP (Fig 3F–H). In biological settings, the activation of latent-TGFβ is likely to occur through an interplay of different mechanisms, for example, depending on the tissue, physiological, or pathophysiological context.

The most established function of fibronectin is to mediate the interaction between cells and various ECM components, therefore acting as a "glue" and a structural component (Mouw *et al*, 2014). The N-terminal part of fibronectin, for example, directly interacts with fibrillins, which is critical for the maturation of ECM fibers and incorporation of latent-TGFβ into ECM stores (Dallas *et al*, 2005). Therefore, cleavage of fibronectin, especially the N-terminus, which we demonstrate is directly cleaved by hepsin *in vitro*, may affect ECM storage of TGFβ and thus TGFβ signaling. It is likely, however, that other proteases also play a role in hepsin-mediated TGFβ signaling *in vivo* as hepsin can activate other proteases, such as MMPs (Reid *et al*, 2017; Wilkinson *et al*, 2017) and serine proteases (Andreasen *et al*, 1997; Moran *et al*, 2006; Reid *et al*, 2017), reported to regulate the cleavage of fibronectin (Moran *et al*, 2006; Borgoño *et al*, 2007; Doucet & Overall, 2011; Zhang *et al*, 2012). Such proteolytic cascades may result, for example, from hepsin-induced downregulation of the general serine protease inhibitor HAI-1 (Tervonen *et al*, 2016). Studies with other proteases capable of cleaving fibronectin have demonstrated that accumulation of fibronectin may lead to alterations of collagen fibers *in vivo* and thus changes in the overall ECM structure (Taylor *et al*, 2015). Whether changes in fibronectin levels, due to the deregulation of hepsin, result in gross structural changes in overall ECM architecture remains to be investigated.

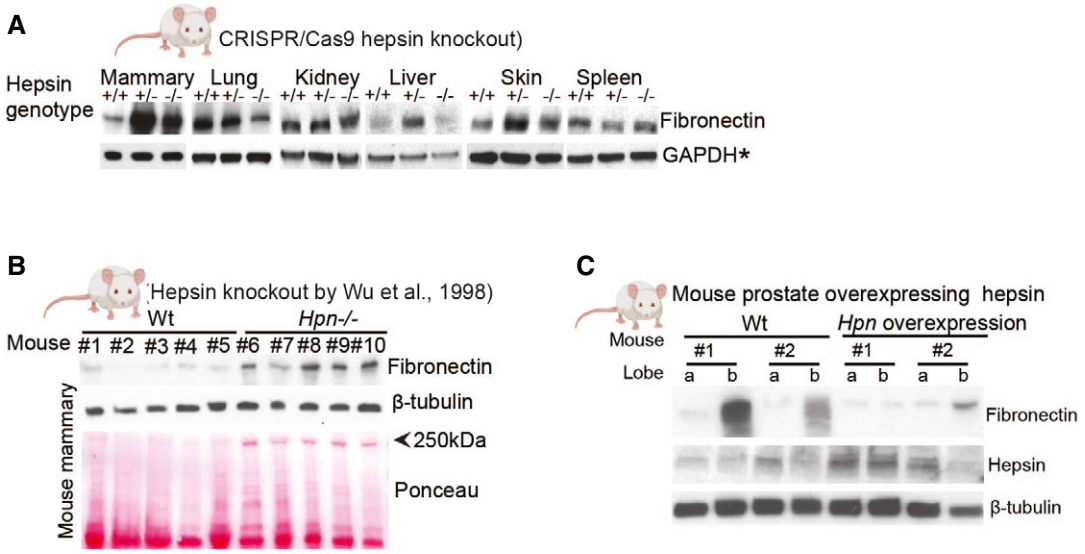

Figure 5. Hepsin reduces fibronectin levels *in vivo*.

A Immunoblot analysis of fibronectin in indicated tissues isolated from Wt, $Hpn^{+/-}$ and $Hpn^{-/-}$ mouse (representative of at least three repeats). *As the same tissue lysates were used as in Fig 1F, the same GAPDH blot is used here as the loading control.

B Immunoblot analysis of fibronectin and β-tubulin (loading control) in lysates from Wt and $Hpn^{-/-}$ mouse mammary tissue ($N = 5$ animals each) from another hepsin knockout mouse model (Wu *et al*, 1998).

C Immunoblot analysis of fibronectin, hepsin, and β-tubulin (loading control) in prostate lysates of control mice or mice with prostate-specific hepsin overexpression (Klezovitch *et al*, 2004). $N = 2$ mice each, the two prostate lobes were run separately (A and B).

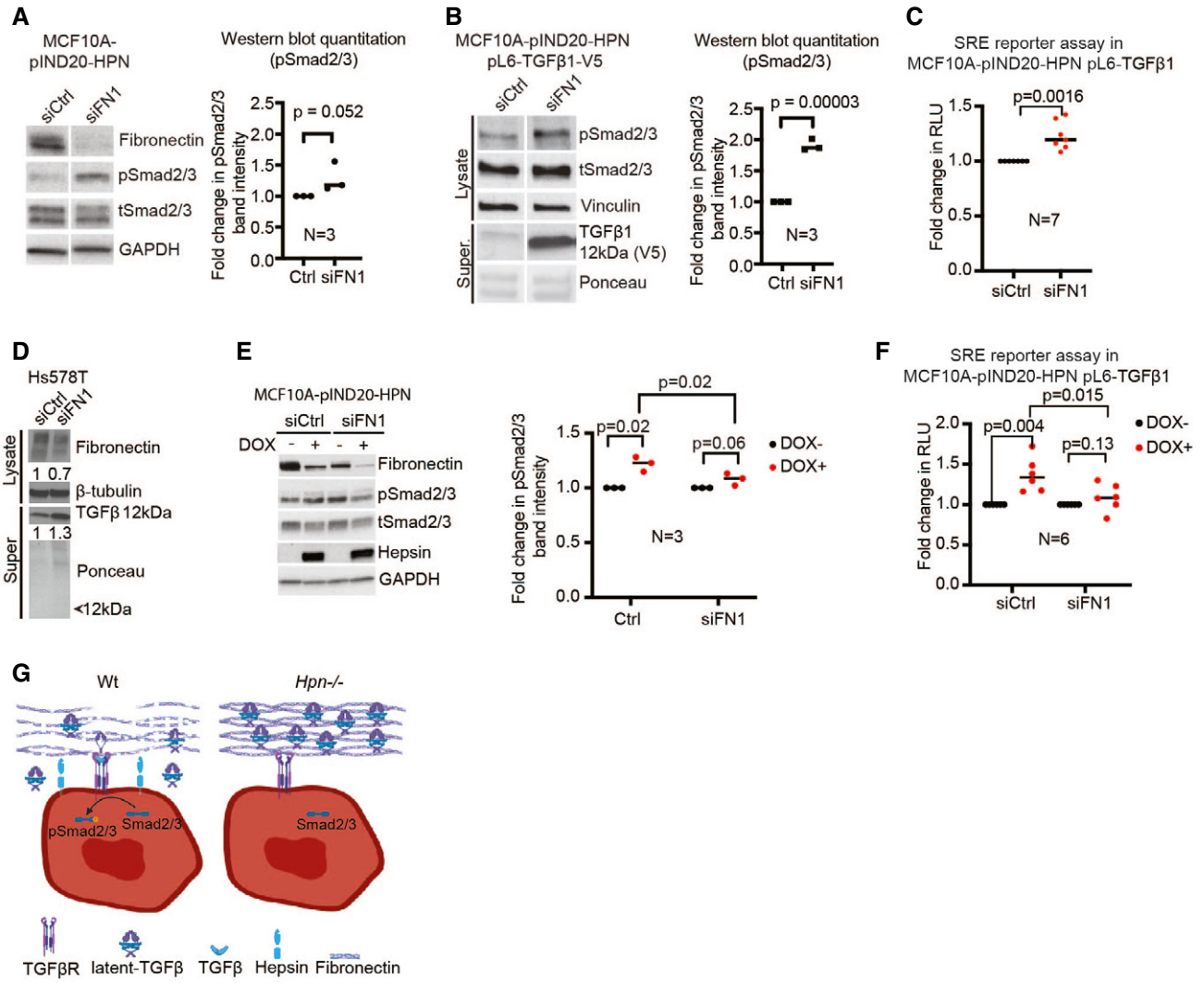

Figure 6. Hepsin-mediated TGFβ1 signaling through the downregulation of fibronectin.

A Immunoblot analysis of fibronectin, pSmad2/3, total Smad2/3, and GAPDH (loading control) in cell lysates from MCF10A-pIND20-HPN cells without hepsin overexpression. The graph depicts quantification of pSmad2/3 normalized to total Smad2/3 levels, compared to siCtrl ($N = 3$ biological repeats).

B Immunoblot analysis of cell lysates (pSmad2/3, total Smad2/3, and vinculin as loading control) and concentrated cell culture supernatant (anti-V5 for TGFβ) from MCF10A-pIND20-HPN pL6-TGFβ1-V5 cells without hepsin overexpression. Ponceau staining is shown as a loading control for the Western blot with concentrated culture supernatant. The graph depicts quantification of pSmad2/3 normalized to total Smad2/3 levels, compared to siCtrl ($N = 3$ biological repeats).

C TGFβ luciferase reporter assay of control or fibronectin silenced MCF10A-pIND20-HPN pL6-TGFβ1 (SRE) TGFβ1 reporter cells with (DOX^+) or without (DOX^-) hepsin overexpression ($N = 7$ biological repeats; Y-axis shows fold change in relative light units (RLU)).

D Immunoblot analysis of cell lysates (fibronectin and β-tubulin (loading control)) and concentrated cell culture supernatant (TGFβ) from Hs578T cells with knockdown of fibronectin. Ponceau staining is shown as the loading control for the Western blot with concentrated culture supernatant. A representative blot from three biological repeats is shown.

E Immunoblot analysis of fibronectin, pSmad2/3, total Smad2/3, hepsin, and GAPDH (loading control) in cell lysates from MCF10A-pIND20-HPN cells with (DOX^+) and without (DOX^-) hepsin overexpression, and with or without fibronectin silencing (siFN1). The graph depicts quantification of pSmad2/3 normalized to total Smad2/3 levels ($N = 3$ biological repeats).

F TGFβ luciferase reporter assay of control or fibronectin silenced MCF10A-pIND20-HPN pL6-TGFβ1 (SRE) TGFβ1 reporter cells, with (DOX^+) and without (DOX^-) hepsin overexpression. ($N = 6$ biological repeats; Y-axis shows fold change in relative light units (RLU)).

G Model figure depicting how hepsin regulates TGFβ signaling. Under Wt conditions, hepsin promotes degradation of fibronectin, which releases latent-TGFβ from ECM stores, thus resulting in the induction of TGFβ signaling. In hepsin knockout mammary glands, TGFβ signaling is compromised as latent-TGFβ cannot be released from ECM stores (Created with BioRender.com). Statistical analyses in (A, B, C, E, F) were done using Student's *t*-test. Data in (A, B, C, E, F) are presented as dot plots where black lines represent the mean.

Source data are available online for this figure.

In conclusion, we show that hepsin mediates the release of latent-TGFβ from the ECM storage specifically in the mammary tissue, which leads to increased TGFβ signaling. This suggests a novel role for hepsin as a mediator between ECM proteolysis and TGFβ growth factor signaling.

Materials and Methods

Reagents

Table 1 lists purified proteins used in this study.

Table 1. Purified proteins used in the study.

Protein	Company	Catalog
Purified plasma fibronectin	Merck	F0895
Fibronectin proteolytic fragment from human plasma, 70 kDa	Merck	F0287
Fibronectin proteolytic fragment from human plasma, 30 kDa	Merck	F9911
Fibronectin 40 kDa α chymotryptic fragment (heparin-binding region)	Merck	F1903
Fibronectin proteolytic fragment from human plasma, 45 kDa	Merck	F0162
Fibronectin 120 kDa α chymotryptic fragment (cell attachment region)	Merck	F1904
hLatent-TGFβ1	CST	#5154
Recombinant human hepsin protein, CF	R&D Systems	4776-SE

Cell lines

All cell lines were regularly tested for mycoplasma contamination. The SUM52PE cell line was a generous donation from Dr. SJ Cook and Dr. PR Gavine (Chell *et al*, 2013) and was cultured in Hams F12 (Invitrogen), insulin 5 μg/ml, hydrocortisone 1 μg/ml, L-glutamine, and antibiotics. All other cell lines were obtained from American Type Culture Collection (ATCC). HMEC-hTERT cell media was MCDB 170 (US Biological) supplemented with insulin 5 μg/ml, bovine pituitary extract (BPE) 70 μg/ml, hydrocortisone 0.5 μl/ml, EGF 5 ng/ml, human transferrin 5 μg/ml, and isoproterenol 0.01 μM and 5% FBS (Biowest). Cell lines MCF7, T47D, MCF10A, and Hs578T were cultured as described in Tervonen *et al,* 2016. MCF12A was cultured in DMEM/F12 (Invitrogen) with 10% FBS (Biowest), EGF 20 ng/ml, hydrocortisone 1 μg/ml, insulin 10 μg/ml, and human transferrin 5 μg/ml. Cell lines HCC70, HCC1395, HCC38, HCC1806, DU4475, HCC1143, HCC1937, and HCC1187 were cultured in RPMI-1640 (Gibco) supplemented with 10% FBS (Biowest), and BT-549 in RPMI-1640 with 10% FBS (Biowest) and 10 μg/ml insulin. The MDA-MB-231 cell line was cultured in Dulbecco's modified Eagle's medium (Sigma), 10% FBS (Biowest); BT-20 and CAMA-1 cell lines were cultured in Eagle's minimum essential medium (Lonza) supplemented with 10% FBS (Biowest). MDA-MB-436 and MDA-MB-453 were cultured in Leibovitz's L-15 Medium (Lonza) with 10% FBS (Biowest).

siRNA knockdown

Fibronectin knockdown was performed with siRNA pool (siTOOLS Biotech) and HIPerFect (Qiagen) transfection reagent, with 100 nM siRNA final concentration. Hs578T cells were switched to serum-free media after transfection, for supernatant analysis. Supernatants were concentrated as described elsewhere (see Mass Spectrometry).

Virus transduction, TGFβ reporter cell lines

Cell line transduction was carried out by incubating plated cells with virus-containing supernatant O/N in the presence of 8 μg/ml of polybrene (MOI = 1). We generated the TGFβ reporter cell lines by transducing MCF10A cells with SRE construct harboring lentivirus particles (MOI=10). Reporter construct virus particles were obtained commercially (Kerafast #FCT228). The luciferase signal was detected by using Pierce™ Firefly Luciferase Glow Assay Kit (Thermo Scientific, PI16177) according to the manufacturer's instructions. Readings were obtained with FLUOstar OMEGA multi-plate reader (BMG LabTech).

Cloning

The pLenti6-TGFβ1-V5 overexpression construct was generated via Gateway cloning from the ORFeome library by the Genome Biology Unit supported by HiLIFE and the Faculty of Medicine, University of Helsinki, and Biocenter Finland.

Tissue, organ weight, and body composition analysis

Carmine alum staining (Sigma, #C1022-5G) of whole mammary glands was performed in inguinal mammary glands from 6-week-old females were spread on glass slips and fixed with Kahle's fixative (Patel *et al*, 2019) O/N at room temperature followed by one wash with 70% ethanol and gradual change to Milli-Q water. Glands were stained with carmine alum O/N, gradually transferred into 100% ethanol, and cleared in xylene. Upon clearing glands were transferred into 100% ethanol, followed by 100% glycerol. The branching was quantitated using ImageJ 1.46r.

H&E staining was performed as described previously (Partanen *et al*, 2012).

Body composition for liquid, fat, and lean mass percentage and organ weight was measured in 6-week-old mice with Bruker minispec LF50 Body Composition Analyzer (Brüker). Statistical significance was derived from a one-sided *t*-test. All the groups had at least $N = 3$.

RNASeq

RNA was extracted from up to 6-week-old mouse mammary glands using hard-tissue beads (Precellys) and TRIzol (Thermo Fisher Scientific). RNA was then DNase treated and purified using RNeasy Mini Kit from Qiagen. Before the library preparation for sequencing, 1 μg of total RNA was treated with NEBNext rRNA Depletion Kit (Human/Mouse/Rat) that removes the ribosomal RNA from the total RNA. The ribosomal depleted RNA was purified with RNeasy mini Elute columns (Qiagen). The absence of rRNA and the quantity of mRNA were measured with Agilent TapeStation 4200. Samples

were sequenced with Illumina NextSeq500 (Illumina, San Diego, CA, USA) at the Biomedicum Functional Genomics Unit, University of Helsinki, using NEBNext Ultra Directional RNA Library Prep Kit. The sequencing was performed as single-end sequencing for read length 75 bp. GSEA analysis and statistical analysis were performed in GSEA 4.0.3 software (Subramanian *et al*, 2005). Gene set clustering was analyzed with Cytoscape (Merico *et al*, 2010). Genomic PCR products were Sanger sequenced (Sequencing Unit at the Finnish Institute for Molecular Medicine, HiLIFE, University of Helsinki and Biocenter Finland) using the same reverse primer used also for genomic PCR (above).

Proteins and hepsin cleavage

Recombinant human hepsin was incubated at various concentrations with 1 μg/μl substrate proteins (latent-TGFβ1, fibronectin fragments) for 1 h, 37°C in PBS, separated on gradient gels and silver stained (GE Healthcare, GE17-1150-01). Silver staining was performed by the Meilahti Clinical Proteomics Core Facility.

Antibodies and inhibitors

The inhibitors and antibodies used in this study were Galunisertib (Selleckchem, S2230), anti-sheep HRP (Upstate cell signaling solutions, #12-342), anti-goat HRP (Millipore, AP106P), anti-rabbit HRP (Millipore, AP132P), anti-mouse (Millipore, AP160P), anti-hepsin (Santa Cruz, sc-33542), anti-hepsin (R&D Systems, AF4776), anti-Fibronectin (Abcam, ab45688), anti-TGFβ1 LAP peptide (Abcam, ab155264), anti- pSmad2/3 (CST#8828), anti-Smad2/3 (CST#8685) anti-TGFβ (CST#3711S), anti-SNAIL (CST#3879S), anti-GAPDH (CST#2118S), anti-β-tubulin (Abcam, ab6046), anti-PAI-1 (Abcam, ab66705), and anti-V5 (Invitrogen, #R96025).

Animal models and experiments

All work and sample isolation from 11-month-old $Hpn^{-/-}$ (Wu *et al*, 1998), 6-month-old LPB-Hepsin (Kasper *et al*, 1998) mice were performed at Lerner Research Institute, Cleveland Clinic, USA; Division of Human Biology, Fred Hutchinson Cancer Research Center, Seattle, USA, respectively.

All mice used for the experiments in Helsinki were housed in individually ventilated cages under the optimal conditions of temperature and humidity. The experiments were conducted according to 3R principles, and animal welfare was regularly monitored.

Wap-Myc mammary/tumor cell isolations were performed like previously described (Partanen *et al*, 2012; Tervonen *et al*, 2016). Experiments were approved by The National Animal Ethics Committee of Finland (ESAVI/3678/04.10.07/2016).

One day before transplantation, Wap-Myc epithelial cells were isolated and transduced with the pInducer21-HPN (Tervonen *et al*, 2016), lentiviral construct, MOI = 10. On transplantation day, 10^5 cells were injected into the cleared fat pads of 3-week-old recipient mice. The experimental mice started receiving doxycycline in drinking water, supplemented with 5% sucrose, 3 days after the transplantation, the control mice received drinking water with sucrose only. Tumors were induced at week 8 by two sequential pregnancies. Mice were sacrificed when the tumor diameter reached 1 cm.

Transplantation experiment of Wt Wap-Myc tumor cells and into Wt and $Hpn^{-/-}$ recipients: 3-week-old Wt FVB recipient mice were obtained from Janvier Labs. Cells were isolated 1 day before transplantation from Wt Wap-Myc tumors and kept in floating culture O/N in growth media (Partanen *et al*, 2012). On transplantation day, viability was estimated with trypan blue, 10^5/gland cells were injected into cleared fat pads of 4-week-old recipient mice (2 glands/mouse). Mice were sacrificed when the tumor diameter reached 2 cm.

Generation of *Hpn* knockout mice by CRISPR/Cas9 editing

gRNAs for *in vivo* CRISPR/Cas9 genome editing were *in vitro* transcribed from mouse genome-wide arrayed lentiviral CRISPR/Cas9 gRNA libraries (Sigma-Aldrich/Merck). Sanger gRNA ID 1822530, target sequence with PAM was 5'-AAGGTGGCAGCTCTCATTGTGG-3' in exon 4 (exon ID: ENSMUSE00001198671). For *in vitro* transcription, primers were from Sigma-Aldrich/Merck and the sequence for gRNA synthesis forward primer was 5'-TAATACGACTCACTATAGA AGGTGGCAGCTCTCA-3' and reverse primer 5'-TTCTAGCTCTAAAA CCAATGAGAGCTGCCACCTT-3'. The gRNA was produced with GeneArt™ Precision gRNA Synthesis Kit (Thermo Fischer Scientific) according to the manufacturer's instructions. Injections into mouse zygotes were performed with the purified gRNA and Cas9 mRNA. Altogether, 209 zygotes were injected, 178 transferred into founding mothers (FVB strain), and 100 live pups were born. Mice were genotyped from ear samples taken after weaning by genomic PCR that was performed with the following primers: forward 5'-TGTCATCGGAAA GGAGTGGC-3' and reverse 5'-GGAGAACAGGCGGGTTGTAA-3' flanking the gRNA-targeting sequence (product length was 493 bp). PCR mix contained a final concentration of 2 mM dNTP mix (Bioline, London, UK), 200 nM of primers (oligos from Sigma-Aldrich/Merck), 1 mM $MgCl_2$, 1 × Phusion HF PCR Buffer (Thermo Fischer Scientific), Phusion High-Fidelity DNA polymerase (Thermo Fischer Scientific), and 2 ng/μl DNA template. Genomic PCR products were Sanger sequenced (Biomedicum Sequencing Unit and Sequencing Unit, FIMM, HiLIFE life science research infrastructures, University of Helsinki and Biocenter Finland) using the same reverse primer used also for genomic PCR (above). We found that 15 mice (16% of live-born F0 cohort) were mutant for *Hpn*. We selected F0 male with 50 bp deletion in *Hpn* exon 4 as a founding father of the strain. This male was paired with wild-type females to obtain F1 generation. The strain was maintained as heterozygotes (no apparent phenotype), which mated to produce wild-type and $Hpn^{-/-}$ littermates.

Acoustic startle reflex (ASR) test

The test is based on Willott *et al* (2003). Shortly, mice were placed in a transparent plastic tube (Ø 4.5 cm, length 8 cm) that was put in the startle chamber (Med Associates) with a background white noise of 65 dB and left undisturbed for 5 min. Acoustic startle stimuli (20-ms white noise bursts) were presented in random order with 8–15 s between the subsequent trials. Altogether, 36 trials with the following noise intensities were randomly applied: 68, 72, 75, 78, 82, 86, 90, 100, and 110 dB. The startle response was recorded for 65 ms starting with the onset of the startle stimulus. The maximum startle amplitude recorded during the 65-ms sampling window was used as the dependent variable and averaged over four trials with given

stimulus intensity. The test was performed by Mouse Behavioral Phenotyping Facility (MBPF) at Neuroscience Center, Helsinki Institute of Life Science (HiLIFE), University of Helsinki and Biocenter Finland (N).

Immunoblot, antibody array, RNA expression analysis, silver staining, and ELISA

Immunoblots were quantitated using ImageJ. Statistical significance was determined via a one-sided *t*-test, unless specified otherwise in the figure legends. All lysates for immunoblot analysis were prepared by lysing cells in PBS-1% Triton X-100 buffer supplemented with Protease Inhibitor Cocktail and Phosphatase inhibitor (Roche). Thereafter, the resulting suspension was incubated on ice for 10 min, centrifuged, and the supernatant collected. Tissue lysates were made in the mentioned lysis buffer by using Precellys 24 tissue homogenizer (Bertin instruments) and the Precellys kit (#KT03961-1-003.2). Proteins were separated on gradient SDS gels (Bio-Rad) and transferred to nitrocellulose membranes (Bio-Rad #1704158). Transfer quality was evaluated with Ponceau staining (Sigma, #P7170). For antibody array experiments, the whole mammary lysates were prepared from 6-week-old virgin females according to the manufacturer's instructions (R&D Systems) and analyzed with Mouse XL Cytokine Antibody Array Kit (RPPA). Signal intensity was quantitated with MATLAB. The proteins from LPB-hepsin prostate samples were extracted from ventral lobes in RIPA buffer (50 mM Tris–HCl pH7.5, 100 mM NaCl, 1% NP-40, 1% Na deoxycholate, 0.1% SDS, 1 mM EDTA, protease/phosphatase inhibitors). The active and total TGFβ ELISA was performed with Human TGF-beta 1 Quantikine ELISA Kit (R&D Systems) according to manufacturer's instructions, except for the activation step, which was substituted with heat activation (Brown *et al*, 1990). In order to detect the absolute levels of TGFβ and not only the active form, we performed hear mediated activation, which liberates the active TGFβ from the small latent complex not detectable by the assay (Brown *et al*, 1990). Readings were obtained with FLUOstar OMEGA multiplate reader (BMG Labtech) at 450 nm.

Mass spectrometry

Culture supernatants were concentrated with Amicon Ultra-0.5 ml 3 K Centrifugal Filters according to the manufacturer's instructions (Millipore). Lysates and supernatants were boiled with lysis buffer with (R)/without β-mercaptoethanol (NR) and separated on gradient gels (Bio-Rad).

Gels were stained o/n RT with Coomassie stain (10% acetic acid, 50% ethanol, Coomassie Brilliant Blue-R250 in MQ), followed by destaining (10% acetic acid, 50% ethanol in MQ).

Bands that were altered by hepsin overexpression (DOX^-/DOX^+) were excised and analyzed by MALDI-TOF as described before (Vaarala *et al*, 2014), and the results were plotted against the proteome of the Mammalian taxon (66651 sequences). Mass spectrometric analysis was performed by the Meilahti Clinical Proteomics Core Facility.

Data availability

The raw RNAseq data for the pIND21-Wap-Myc tumors GSE164510 (https://www.ncbi.nlm.nih.gov/geo/query/acc.cgi?acc = GSE164510), Hpn wild-type, and knockout mammary glands GSE164509 (https://www.ncbi.nlm.nih.gov/geo/query/acc.cgi?acc = GSE164509) are publically available at the GEO repository.

Expanded View for this article is available online.

Acknowledgements
We are grateful to Biomedicum Functional Genomics Unit/Libraries (FuGU/Libraries), Finnish Genome Editing Center (FinGEEC), Biomedicum Virus Core Unit (BVC), Genome Biology Unit (GBU) and Biomedicum Imaging Unit (BIU), Meilahti Clinical Proteomics Core Facility, and Laboratory Animal Center (LAC) (all from HiLIFE, University of Helsinki and Biocenter Finland) for their services. We the Klefström laboratory personnel for discussions and critical comments on the manuscript. We thank for the technical assistance provided by M. Merisalo-Soikkeli, K. Karjalainan, and T.Välimäki. We thank for financial support the Finnish Cancer Institute (FCI). This work was funded by grants from The Academy of Finland, Business Finland, EU H2020 RESCUER, Archimedes Foundation, Ida Montinin Foundation, Cancer Society of Finland, Finnish Cancer Organizations, Sigrid Juselius Foundation, K. Albin Johanssons stiftelse, Jane and Aatos Erkko Foundation, and iCAN Digital Precision Cancer Medicine Flagship. T.A.T. was funded by the Helsinki Institute of Life Science Infrastructures (HiLIFE) of the University of Helsinki.

Author contributions
DB conceptualized; provided resources; curated the data; involved in formal analysis; investigated; contributed to methodology; and wrote the original draft, review, and editing. SMP provided resources; curated data; validated; investigated; contributed to methodology; and wrote the original draft, review, editing, and illustrations. PM conceptualized; provided resources; curated the data; involved in formal analysis; investigated the study; contributed to methodology; and wrote the original draft. IS involved in formal analysis; visualized the study; and wrote the original draft. KB curated the data; involved in formal analysis; investigated the study; contributed to methodology; and wrote the original draft. H-AH provided resources and methodology. JE provided resources and methodology, and wrote the original draft. TR provided resources and methodology. OK, VV, SL, and QW provided resources and wrote the original draft. OM, SK, and PL provided resources, curated the data, involved in funding acquisition, and wrote the original draft. JP conceptualized the study; involved in funding acquisition; visualized the study; contributed to methodology; and wrote the original draft, review, and editing. TT conceptualized the study; provided resources; curated the data; involved in formal analysis; supervised the study; involved in funding acquisition; investigated the study; visualized the study; contributed to methodology; wrote the original draft; and contributed to project administration, review, and editing. JK conceptualized the study; provided resources; curated the data; involved in formal analysis; supervised the study; involved in funding acquisition; validated the study; investigated the study, visualized the study; contributed to methodology; wrote the original draft; involved in project administration; review and editing.

Conflict of interest
Dr. Klefström's research projects received funding from AbbVie, Orion Pharma, and Roche/Genentech. Dr. Klefström has served as a member of scientific advisory board or consultant to AbbVie, Astra-Zeneca, MSD, Orion Pharma, Pfizer, Roche/Genentech, and UPM Biomedicals. Dr. Pouwels has consulted for Biomedicum Genomics. Other authors declare no conflicts of interest.

References

Andreasen PA, Kjøller L, Christensen L, Duffy MJ (1997) The urokinase-type plasminogen activator system in cancer metastasis: a review. *Int J cancer* 72: 1 – 22

Antalis TM, Buzza MS, Hodge KM, Hooper JD, Netzel-Arnett S (2010) The cutting edge: membrane-anchored serine protease activities in the pericellular microenvironment. *Biochem J* 428: 325 – 346

Beaufort N, Scharrer E, Kremmer E, Lux V, Ehrmann M, Huber R, Houlden H, Werring D, Haffner C, Dichgans M (2014) Cerebral small vessel disease-related protease HtrA1 processes latent TGF-β binding protein 1 and facilitates TGF-β signaling. *Proc Natl Acad Sci USA* 111: 16496 – 16501

Bellomo C, Caja L, Moustakas A (2016) Transforming growth factor β as regulator of cancer stemness and metastasis. *Br J Cancer* 115: 761 – 769

Borgoño CA, Michael IP, Shaw JLV, Luo L-Y, Ghosh MC, Soosaipillai A, Grass L, Katsaros D, Diamandis EP (2007) Expression and functional characterization of the cancer-related serine protease, human tissue kallikrein 14. *J Biol Chem* 282: 2405 – 2422

Brionne TC, Tesseur I, Masliah E, Wyss-Coray T (2003) Loss of TGF-beta 1 leads to increased neuronal cell death and microgliosis in mouse brain. *Neuron* 40: 1133 – 1145

Brown PD, Wakefield LM, Levinson AD, Sporn MB (1990) Physicochemical activation of recombinant latent transforming growth factor-beta's 1, 2, and 3. *Growth Factors* 3: 35 – 43

Chang C, Werb Z (2001) The many faces of metalloproteases: cell growth, invasion, angiogenesis and metastasis. *Trends Cell Biol* 11: S37 – S43

Chell V, Balmanno K, Little AS, Wilson M, Andrews S, Blockley L, Hampson M, Gavine PR, Cook SJ (2013) Tumour cell responses to new fibroblast growth factor receptor tyrosine kinase inhibitors and identification of a gatekeeper mutation in FGFR3 as a mechanism of acquired resistance. *Oncogene* 32: 3059 – 3070

Chen Z, Fan Z, McNeal JE, Nolley R, Caldwell MC, Mahadevappa M, Zhang Z, Warrington JA, Stamey TA (2003) Hepsin and maspin are inversely expressed in laser capture microdissectioned prostate cancer. *J Urol* 169: 1316 – 1319

Cichon MA, Moruzzi ME, Shqau TA, Miller E, Mehner C, Ethier SP, Copland JA, Radisky ES, Radisky DC (2016) MYC is a crucial mediator of TGFβ-induced invasion in basal breast cancer. *Cancer Res* 76: 3520 – 3530

Dallas SL, Sivakumar P, Jones CJP, Chen Q, Peters DM, Mosher DF, Humphries MJ, Kielty CM (2005) Fibronectin regulates latent transforming growth factor-beta (TGF beta) by controlling matrix assembly of latent TGF beta-binding protein-1. *J Biol Chem* 280: 18871 – 18880

Damalanka VC, Han Z, Karmakar P, O'Donoghue AJ, La Greca F, Kim T, Pant SM, Helander J, Klefström J, Craik CS *et al* (2019) Discovery of selective matriptase and Hepsin serine protease inhibitors: useful chemical tools for cancer cell biology. *J Med Chem* 62: 480 – 490

Del Rosso M, Fibbi G, Pucci M, D'Alessio S, Del Rosso A, Magnelli L, Chiarugi V (2002) Multiple pathways of cell invasion are regulated by multiple families of serine proteases. *Clin Exp Metastasis* 19: 193 – 207

Derynck R, Budi EH (2019) Specificity, versatility, and control of TGF-β family signaling. *Sci Signal* 12: eaav5183

Dhanasekaran SM, Barrette TR, Ghosh D, Shah R, Varambally S, Kurachi K, Pienta KJ, Rubin MA, Chinnaiyan AM (2001) Delineation of prognostic biomarkers in prostate cancer. *Nature* 412: 822 – 826

Dickson MC, Martin JS, Cousins FM, Kulkarni AB, Karlsson S, Akhurst RJ (1995) Defective haematopoiesis and vasculogenesis in transforming growth factor-beta 1 knock out mice. *Development* 121: 1845 – 1854

ten Dijke P, Arthur HM (2007) Extracellular control of TGFbeta signalling in vascular development and disease. *Nat Rev Mol Cell Biol* 8: 857 – 869

Doucet A, Overall CM (2011) Broad coverage identification of multiple proteolytic cleavage site sequences in complex high molecular weight proteins using quantitative proteomics as a complement to edman sequencing. *Mol Cell Proteomics* 10: M110.003533

Ernst T, Hergenhahn M, Kenzelmann M, Cohen CD, Bonrouhi M, Weninger A, Klären R, Gröne EF, Wiesel M, Güdemann C *et al* (2002) Decrease and gain of gene expression are equally discriminatory markers for prostate carcinoma: a gene expression analysis on total and microdissected prostate tissue. *Am J Pathol* 160: 2169 – 2180

Ewan KB, Shyamala G, Ravani SA, Tang Y, Akhurst R, Wakefield L, Barcellos-Hoff MH (2002) Latent transforming growth factor-beta activation in mammary gland: regulation by ovarian hormones affects ductal and alveolar proliferation. *Am J Pathol* 160: 2081 – 2093

Fontana L, Chen Y, Prijatelj P, Sakai T, Fässler R, Sakai LY, Rifkin DB (2005) Fibronectin is required for integrin alphavbeta6-mediated activation of latent TGF-beta complexes containing LTBP-1. *FASEB J Off Publ Fed Am Soc Exp Biol* 19: 1798 – 1808

Fukushima T, Uchiyama S, Tanaka H, Kataoka H (2018) Hepatocyte growth factor activator: a proteinase linking tissue injury with repair. *Int J Mol Sci* 19: 3435

Ganesan R, Kolumam GA, Lin SJ, Xie M-H, Santell L, Wu TD, Lazarus RA, Chaudhuri A, Kirchhofer D (2011) Proteolytic activation of pro-macrophage-stimulating protein by hepsin. *Mol Cancer Res* 9: 1175 – 1186

Ganesan R, Zhang Y, Landgraf KE, Lin SJ, Moran P, Kirchhofer D (2012) An allosteric anti-hepsin antibody derived from a constrained phage display library. *Protein Eng Des Sel* 25: 127 – 133

Ge G, Greenspan DS (2006) BMP1 controls TGFbeta1 activation via cleavage of latent TGFbeta-binding protein. *J Cell Biol* 175: 111 – 120

Green KA, Lund LR (2005) ECM degrading proteases and tissue remodelling in the mammary gland. *BioEssays* 27: 894 – 903

Guipponi M, Tan J, Cannon PZF, Donley L, Crewther P, Clarke M, Wu Q, Shepherd RK, Scott HS (2007) Mice deficient for the type II transmembrane serine protease, TMPRSS1/hepsin, exhibit profound hearing loss. *Am J Pathol* 171: 608 – 616

Herter S, Piper D, Aaron W, Gabriele T, Cutler G, Cao P, Bhatt A, Choe Y, Craik C, Walker N *et al* (2005) Hepatocyte growth factor is a preferred *in vitro* substrate for human hepsin, a membrane-anchored serine protease implicated in prostate and ovarian cancers. *Biochem J* 390: 125 – 136

Higashiyama S, Nanba D, Nakayama H, Inoue H, Fukuda S (2011) Ectodomain shedding and remnant peptide signalling of EGFRs and their ligands. *J Biochem* 150: 15 – 22

Hooper JD, Clements JA, Quigley JP, Antalis TM (2001) Type II transmembrane serine proteases. Insights into an emerging class of cell surface proteolytic enzymes. *J Biol Chem* 276: 857 – 860

Hsu Y-C, Huang H-P, Yu I-S, Su K-Y, Lin S-R, Lin W-C, Wu H-L, Shi G-Y, Tao M-H, Kao C-H *et al* (2012) Serine protease hepsin regulates hepatocyte size and hemodynamic retention of tumor cells by hepatocyte growth factor signaling in mice. *Hepatology* 56: 1913 – 1923

Ingman WV, Robertson SA (2008) Mammary gland development in transforming growth factor beta1 null mutant mice: systemic and epithelial effects. *Biol Reprod* 79: 711 – 717

Jenkins G (2008) The role of proteases in transforming growth factor-beta activation. *Int J Biochem Cell Biol* 40: 1068 – 1078

Kasper S, Sheppard PC, Yan Y, Pettigrew N, Borowsky AD, Prins GS, Dodd JG, Duckworth ML, Matusik RJ (1998) Development, progression, and androgen-dependence of prostate tumors in probasin-large T antigen transgenic mice: a model for prostate cancer. *Lab Invest* 78: i – xv

Klezovitch O, Chevillet J, Mirosevich J, Roberts RL, Matusik RJ, Vasioukhin V (2004) Hepsin promotes prostate cancer progression and metastasis. *Cancer Cell* 6: 185 – 195

Koschubs T, Dengl S, Dürr H, Kaluza K, Georges G, Hartl C, Jennewein S, Lanzendörfer M, Auer J, Stern A *et al* (2012) Allosteric antibody inhibition of human hepsin protease. *Biochem J* 442: 483 – 494

Kulkarni AB, Huh CG, Becker D, Geiser A, Lyght M, Flanders KC, Roberts AB, Sporn MB, Ward JM, Karlsson S (1993) Transforming growth factor beta 1 null mutation in mice causes excessive inflammatory response and early death. *Proc Natl Acad Sci USA* 90: 770 – 774

Li S, Peng J, Wang H, Zhang W, Brown JM, Zhou Y, Wu Q (2020) Hepsin enhances liver metabolism and inhibits adipocyte browning in mice. *Proc Natl Acad Sci USA* 117: 12359 – 12367

Liu R-M, Desai LP (2015) Reciprocal regulation of TGF-β and reactive oxygen species: A perverse cycle for fibrosis. *Redox Biol* 6: 565 – 577

Lu P, Takai K, Weaver VM, Werb Z (2011) Extracellular matrix degradation and remodeling in development and disease. *Cold Spring Harb Perspect Biol* 3: a005058

Luo J, Duggan DJ, Chen Y, Sauvageot J, Ewing CM, Bittner ML, Trent JM, Isaacs WB (2001) Human prostate cancer and benign prostatic hyperplasia: molecular dissection by gene expression profiling. *Cancer Res* 61: 4683 – 4688

Lyons RM, Keski-Oja J, Moses HL (1988) Proteolytic activation of latent transforming growth factor-beta from fibroblast-conditioned medium. *J Cell Biol* 106: 1659 – 1665

Lyons RM, Gentry LE, Purchio AF, Moses HL (1990) Mechanism of activation of latent recombinant transforming growth factor beta 1 by plasmin. *J Cell Biol* 110: 1361 – 1367

Magee JA, Araki T, Patil S, Ehrig T, True L, Humphrey PA, Catalona WJ, Watson MA, Milbrandt J (2001) Expression profiling reveals hepsin overexpression in prostate cancer. *Cancer Res* 61: 5692 – 5696

Mamuya FA, Duncan MK (2012) aV integrins and TGF-β-induced EMT: a circle of regulation. *J Cell Mol Med* 16: 445 – 455

Mariathasan S, Turley SJ, Nickles D, Castiglioni A, Yuen K, Wang Y, Kadel EE III, Koeppen H, Astarita JL, Cubas R *et al* (2018) TGFβ attenuates tumour response to PD-L1 blockade by contributing to exclusion of T cells. *Nature* 554: 544 – 548

Merico D, Isserlin R, Stueker O, Emili A, Bader GD (2010) Enrichment map: a network-based method for gene-set enrichment visualization and interpretation. *PLoS One* 5: e13984

Miao J, Mu D, Ergel B, Singavarapu R, Duan Z, Powers S, Oliva E, Orsulic S (2008) Hepsin colocalizes with desmosomes and induces progression of ovarian cancer in a mouse model. *Int J cancer* 123: 2041 – 2047

Miyazono K, Hellman U, Wernstedt C, Heldin CH (1988) Latent high molecular weight complex of transforming growth factor beta 1. Purification from human platelets and structural characterization. *J Biol Chem* 263: 6407 – 6415

Mohammed FF, Khokha R (2005) Thinking outside the cell: proteases regulate hepatocyte division. *Trends Cell Biol* 15: 555 – 563

Moran P, Li W, Fan B, Vij R, Eigenbrot C, Kirchhofer D (2006) Pro-urokinase-type plasminogen activator is a substrate for hepsin. *J Biol Chem* 281: 30439 – 30446

Moses H, Barcellos-Hoff MH (2011) TGF-beta biology in mammary development and breast cancer. *Cold Spring Harb Perspect Biol* 3: a003277

Mouw JK, Ou G, Weaver VM (2014) Extracellular matrix assembly: a multiscale deconstruction. *Nat Rev Mol Cell Biol* 15: 771 – 785

Neptune ER, Frischmeyer PA, Arking DE, Myers L, Bunton TE, Gayraud B, Ramirez F, Sakai LY, Dietz HC (2003) Dysregulation of TGF-beta activation contributes to pathogenesis in Marfan syndrome. *Nat Genet* 33: 407 – 411

Olinger E, Lake J, Sheehan S, Schiano G, Takata T, Tokonami N, Debaix H, Consolato F, Rampoldi L, Korstanje R *et al* (2019) Hepsin-mediated processing of uromodulin is crucial for salt-sensitivity and thick ascending limb homeostasis. *Sci Rep* 9: 12287

Overall CM, Blobel CP (2007) In search of partners: linking extracellular proteases to substrates. *Nat Rev Mol Cell Biol* 8: 245 – 257

Pant SM, Belitskin D, Ala-Hongisto H, Klefström J, Tervonen TA (2018a) Analyzing the type II transmembrane serine protease hepsin-dependent basement membrane remodeling in 3D cell culture. *Methods Mol Biol* 1731: 169 – 178

Pant SM, Mukonoweshuro A, Desai B, Ramjee MK, Selway CN, Tarver GJ, Wright AG, Birchall K, Chapman TM, Tervonen TA *et al* (2018b) Design, synthesis, and testing of potent, selective hepsin inhibitors via application of an automated closed-loop optimization platform. *J Med Chem* 61: 4335 – 4347

Partanen JI, Tervonen TA, Myllynen M, Lind E, Imai M, Katajisto P, Dijkgraaf GJP, Kovanen PE, Makela TP, Werb Z *et al* (2012) Tumor suppressor function of Liver kinase B1 (Lkb1) is linked to regulation of epithelial integrity. *Proc Natl Acad Sci USA* 109: E388 – E397

Patel Y, Soni M, Awgulewitsch A, Kern MJ, Liu S, Shah N, Singh UP, Chen H (2019) Overexpression of miR-489 derails mammary hierarchy structure and inhibits HER2/neu-induced tumorigenesis. *Oncogene* 38: 445 – 453

Proetzel G, Pawlowski SA, Wiles MV, Yin M, Boivin GP, Howles PN, Ding J, Ferguson MWJ, Doetschman T (1995) Transforming growth factor–β3 is required for secondary palate fusion. *Nat Genet* 11: 409 – 414

Quarto N, Leonard B, Li S, Marchand M, Anderson E, Behr B, Francke U, Reijo-Pera R, Chiao E, Longaker MT (2012) Skeletogenic phenotype of human Marfan embryonic stem cells faithfully phenocopied by patient-specific induced-pluripotent stem cells. *Proc Natl Acad Sci USA* 109: 215 – 220

Reid JC, Matsika A, Davies CM, He Y, Broomfield A, Bennett NC, Magdolen V, Srinivasan B, Clements JA, Hooper JD (2017) Pericellular regulation of prostate cancer expressed kallikrein-related peptidases and matrix metalloproteinases by cell surface serine proteases. *Am J Cancer Res* 7: 2257 – 2274

Robertson IB, Horiguchi M, Zilberberg L, Dabovic B, Hadjiolova K, Rifkin DB (2015) Latent TGF-β-binding proteins. *Matrix Biol* 47: 44 – 53

Robertson IB, Rifkin DB (2016) Regulation of the bioavailability of TGF-β and TGF-β-related proteins. *Cold Spring Harb Perspect Biol* 8: a021907

Sanford LP, Ormsby I, Gittenberger-de Groot AC, Sariola H, Friedman R, Boivin GP, Cardell EL, Doetschman T (1997) TGFbeta2 knockout mice have multiple developmental defects that are non-overlapping with other TGFbeta knockout phenotypes. *Development* 124: 2659 – 2670

Sato Y, Rifkin DB (1989) Inhibition of endothelial cell movement by pericytes and smooth muscle cells: activation of a latent transforming growth factor-beta 1-like molecule by plasmin during co-culture. *J Cell Biol* 109: 309 – 315

Shull MM, Ormsby I, Kier AB, Pawlowski S, Diebold RJ, Yin M, Allen R, Sidman C, Proetzel G, Calvin D (1992) Targeted disruption of the mouse transforming growth factor-beta 1 gene results in multifocal inflammatory disease. *Nature* 359: 693 – 699

Sounni NE, Dehne K, van Kempen L, Egeblad M, Affara NI, Cuevas I, Wiesen J, Junankar S, Korets L, Lee J *et al* (2010) Stromal regulation of vessel stability by MMP14 and TGFbeta. *Dis Model Mech* 3: 317 – 332

Stamey TA, Warrington JA, Caldwell MC, Chen Z, Fan Z, Mahadevappa M, McNeal JE, Nolley R, Zhang Z (2001) Molecular genetic profiling of Gleason grade 4/5 prostate cancers compared to benign prostatic hyperplasia. *J Urol* 166: 2171 – 2177

Stephan C, Yousef GM, Scorilas A, Jung K, Jung M, Kristiansen G, Hauptmann S, Kishi T, Nakamura T, Loening SA *et al* (2004) Hepsin is highly over expressed in and a new candidate for a prognostic indicator in prostate cancer. *J Urol* 171: 187 – 191

Subramanian A, Tamayo P, Mootha VK, Mukherjee S, Ebert BL, Gillette MA, Paulovich A, Pomeroy SL, Golub TR, Lander, ES, *et al* (2005) Gene set enrichment analysis: a knowledge-based approach for interpreting genome-wide expression profiles. *Proc Natl Acad Sci USA* 25: 15545 – 15550

Tanimoto H, Yan Y, Clarke J, Korourian S, Shigemasa K, Parmley TH, Parham GP, O'Brien TJ (1997) Hepsin, a cell surface serine protease identified in hepatoma cells, is overexpressed in ovarian cancer. *Cancer Res* 57: 2884 – 2887

Tauriello DVF, Palomo-Ponce S, Stork D, Berenguer-Llergo A, Badia-Ramentol J, Iglesias M, Sevillano M, Ibiza S, Cañellas A, Hernando-Momblona X *et al* (2018) TGFβ drives immune evasion in genetically reconstituted colon cancer metastasis. *Nature* 554: 538 – 543

Taylor SH, Yeung C-Y, Kalson NS, Lu Y, Zigrino P, Starborg T, Warwood S, Holmes DF, Canty-Laird EG, Mauch C *et al* (2015) Matrix metalloproteinase 14 is required for fibrous tissue expansion. *eLife* 4: e09345

Tervonen TA, Belitškin D, Pant SM, Englund JI, Marques E, Ala-Hongisto H, Nevalaita L, Sihto H, Heikkilä P, Leidenius M *et al* (2016) Deregulated hepsin protease activity confers oncogenicity by concomitantly augmenting HGF/MET signalling and disrupting epithelial cohesion. *Oncogene* 35: 1832 – 1846

Tripathi M, Nandana S, Yamashita H, Ganesan R, Kirchhofer D, Quaranta V (2008) Laminin-332 is a substrate for hepsin, a protease associated with prostate cancer progression. *J Biol Chem* 283: 30576 – 30584

Utz B, Turpin R, Lampe J, Pouwels J, Klefström J (2020) Assessment of the WAP-Myc mouse mammary tumor model for spontaneous metastasis. *Sci Rep* 10: 18733

Vaarala O, Vuorela A, Partinen M, Baumann M, Freitag TL, Meri S, Saavalainen P, Jauhiainen M, Soliymani R, Kirjavainen T *et al* (2014) Antigenic differences between AS03 adjuvanted influenza A (H1N1) pandemic vaccines: implications for pandemrix-associated narcolepsy risk. *PLoS One* 9: e114361

Welsh JB, Sapinoso LM, Su AI, Kern SG, Wang-Rodriguez J, Moskaluk CA, Frierson HFJ, Hampton GM (2001) Analysis of gene expression identifies candidate markers and pharmacological targets in prostate cancer. *Cancer Res* 61: 5974 – 5978

Wilkinson DJ, Desilets A, Lin H, Charlton S, Del Carmen Arques M, Falconer A, Bullock C, Hsu Y-C, Birchall K, Hawkins A *et al* (2017) The serine proteinase hepsin is an activator of pro-matrix metalloproteinases: molecular mechanisms and implications for extracellular matrix turnover. *Sci Rep* 7: 16693

Willott JF, Tanner L, O'Steen J, Johnson KR, Bogue MA, Gagnon L (2003) Acoustic startle and prepulse inhibition in 40 inbred strains of mice. *Behav Neurosci* 117: 716 – 727

Wiseman BS, Sternlicht MD, Lund LR, Alexander CM, Mott J, Bissell MJ, Soloway P, Itohara S, Werb Z (2003) Site-specific inductive and inhibitory activities of MMP-2 and MMP-3 orchestrate mammary gland branching morphogenesis. *J Cell Biol* 162: 1123 – 1133

Wu Q, Yu D, Post J, Halks-Miller M, Sadler JE, Morser J (1998) Generation and characterization of mice deficient in hepsin, a hepatic transmembrane serine protease. *J Clin Invest* 101: 321 – 326

Yeung T-L, Leung CS, Wong K-K, Samimi G, Thompson MS, Liu J, Zaid TM, Ghosh S, Birrer MJ, Mok SC (2013) TGF-β modulates ovarian cancer invasion by upregulating CAF-derived versican in the tumor microenvironment. *Cancer Res* 73: 5016 – 5028

Yu Q, Stamenkovic I (2000) Cell surface-localized matrix metalloproteinase-9 proteolytically activates TGF-beta and promotes tumor invasion and angiogenesis. *Genes Dev* 14: 163 – 176

Zhang X, Chen CT, Bhargava M, Torzilli PA (2012) A comparative study of fibronectin cleavage by MMP-1, -3, -13, and -14. *Cartilage* 3: 267 – 277

